Advances in Geo-Energy Research

Vol. 12, No. 1, p. 22-34, 2024

Original article

Enhancement of oil transport through nanopores via cation exchange in thin brine films at rock-oil interface

XiangYu Hong[1], Xu Jin[2]*, Man Shen[2], JingCun Fan[1], HengAn Wu[1], FengChao Wang[1]*

[1]*CAS Key Laboratory of Mechanical Behavior and Design of Materials, Department of Modern Mechanics, University of Science and Technology of China, Hefei 230027, P. R. China*

[2]*PetroChina Research Institute of Petroleum Exploration & Development, Beijing 100083, P. R. China*

Keywords:
Oil/brine/rock interactions
oil transport
brine films
cation exchange
molecular dynamics simulation

Cited as:
Hong, X., Jin, X., Shen, M., Fan, J., Wu, H., Wang, F. Enhancement of oil transport through nanopores via cation exchange in thin brine films at rock-oil interface. Advances in Geo-Energy Research, 2024, 12(1): 22-34.
https://doi.org/10.46690/ager.2024.04.03

Abstract:
Interactions at the oil/brine/rock interfaces play a pivotal role in the mobility of crude oil within reservoir matrices. Unraveling the microscopic mechanisms of these interactions is crucial for ion-engineered water flooding in secondary and tertiary oil recovery. In this study, the occurrence and transport behavior of crude oil in kaolinite nanopores covered with thin brine films was investigated by molecular dynamics simulation. There is an apparent interface layered phenomenon for the liquid molecules in slit pores and the polar oil components primarily concentrate at the oil/brine interfacial region and form various binding connections with ions. The interfacial interactions between the polar oil components and brine ions exhibit an inhibitory effect on the transport of crude oil through nanopores. The interaction mechanism between acetic acid molecules and hydrated ions was elucidated by interaction modes and interaction intensity, which was proved to illustrate the flow difference in different brine film systems. Moreover, a strategy of exchanging the binding sites of divalent cations with acetic acid molecules by monovalent cations with a higher concentration was proposed. The cation exchange scheme was further validated, demonstrating an enhancement in the oil mobility within nanopores. These findings deepen our understanding of oil/brine/rock interfacial interactions and provide a significant molecular perspective on ion-engineered water flooding for enhanced oil recovery.

1. Introduction

With the rapid development of global economics, the demand for crude oil has been increasing year by year as a significant fuel and chemical raw material. In recent years, unconventional oil/gas resources are gradually becoming strategic alternatives to conventional oil and gas resources for their huge reserves and wide distribution in the world (Zou et al., 2015; Feng et al., 2020; Cai et al., 2022). However, unconventional reservoir contains various micro and nano pores with low permeability and porosity (Zhang et al., 2020), as shown in Fig. 1(a). The strong rock/oil interfacial interactions under confined situations make a poor mobility for crude oil (Jiang et al., 2018, 2020).

The geological exploring data have proved that the reservoir matrixes are filled with formation water before the crude oil migrates into rock pores (Koleini et al., 2019b). When the water is drained by crude oil from the rock pores, there is still a water film spreading onto the rock surfaces because of the intrinsic water-wet characteristics (Mohammed and Babadagli, 2015). The water film plays a role in connecting the oil phase and rock surface, as shown in Fig. 1(b). In addition, due to the geological interaction and mineral dissolution over a long period of time (Myint and Firoozabadi, 2015), there are various types of ions in the formation water, which can form complicated ionic complex with the polar oil components like asphaltene and carboxylic acid in the rock/water/oil interfacial region (Denton et al., 2019), as shown in Fig. 1(c). The adsorption of polar components can further enhance the adhesion of oil on the rock surface, even resulting in the

*Corresponding author.
E-mail address: xyhong97@mail.ustc.edu.cn (X. Hong); jinxu@petrochina.com.cn (X. Jin); shenman0106@petrochina.com.cn (M. Shen); fanjc@ustc.edu.cn (J. Fan); wuha@ustc.edu.cn (H. Wu); wangfc@ustc.edu.cn (F. Wang).

Received January 27, 2024; revised February 14, 2024; accepted March 1, 2024; available online March 5, 2024.

Yandy Scientific Press

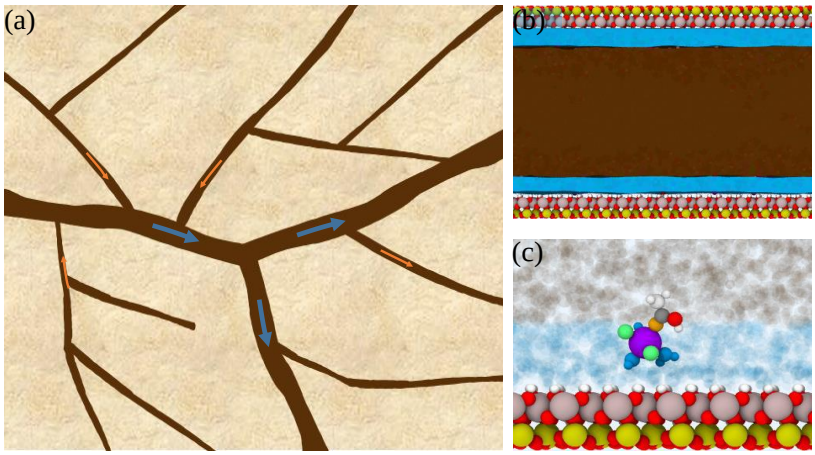

Fig. 1. (a) The flow schematic diagram of crude oil in the micro and nano pores, (b) the simplified pore model involved in oil/brine/rock three phase systems. The blue and black regions represent the brine films and oil phase, respectively, (c) the binding connection between the polar oil component and hydrated ions at the oil/brine interface.

wettability alteration of rock surface (Shaik et al., 2020). In recent years, it has been proved that the thin brine film has an important impact on the rock/oil interfacial interactions (Guo et al., 2020), including electrical double layer expansion, ion exchange, pinning point, screening effect and so on (Koleini et al., 2021). Whatever, the brine films establish a linkage between the nonpolar components of crude oil and rock surface through the adsorption of polar components (Mahmoudvand et al., 2019). In particular, the cations in brine films play an important role in the adsorption of polar components on rock surfaces (Underwood et al., 2015). Over the years, ion binding interactions were widely identified in different oil and brine samples despite of the fact that the composition of crude oil, brine and rock surface can bring some uncertainties of mechanistic study on the oil/brine/rock interaction (Buckley et al., 1998). Furthermore, four potential interaction mechanisms for crude oil adsorption on rock surfaces linked with cations including cation exchange, ligand exchange, cation bridging and water bridging were proposed (Underwood et al., 2015; Lin et al., 2018). With the prevalence of low salinity water flooding technology in the past years, some specific ion combination of injection brine was proved to be able to weaken the rock/oil interactions and enhance oil recovery, which is also denoted as ion-engineered water flooding or smart water flooding (Kilybay et al., 2017). For example, the combination of SO_4^{2-} and Mg^{2+} or SO_4^{2-} and Ca^{2+} can make the carbonate rock surfaces more hydrophilic and enhance the recovery efficiency (Moosavi et al., 2019). It was also reported that Mg^{2+} can displace the Ca^{2+} binding with carboxylate from the surface owing to its more potent affinity to carboxylate (Bai et al., 2021). Due to the complexity introduced by the injected multicomponent brine solution, which can disrupt the initial thermodynamic equilibrium condition at the oil/brine/rock interface, the mechanisms underlying ion-engineered water flooding are recognized as a combination of multiple factors rather than a singular one (Buckley et al., 1998; Koleini et al., 2021). Among these potential mechanisms, multicomponent ion exchange was widely recognized as one of the main mechanisms (Bai et al., 2021). Multicomponent ion exchange mechanism is based on a competitive effect of the interaction strength among polar oil components, ions and rock surface (Wang et al., 2023). Thus, the interaction strength characterization of oil/brine/rock interface is both essential for whether the mechanistic study on oil/brine/rock interfacial interaction or enhanced oil recovery.

At present, there are several prevailing experimental methods to measure the interaction strength of brine/oil interface such as surface tension measurement (Chakravarty et al., 2015), atomic force microscope measurement (Hu et al., 2021). Nevertheless, discrepancies persist in the literature regarding the interfacial interaction between distinct brine films and oil (Umadevi and Senthilkumar, 2014; Chakravarty et al., 2015). Furthermore, the molecular-level interaction mechanisms between brine ions and polar components in nanopores remain inadequately understood. In recent years, the molecular dynamics simulation has emerged as a robust and effective tool in the field of material and interface science (Wang and Wu, 2013; Chu and Zhang, 2023; Wu et al., 2024). Concurrently, there has been significant growth in atomic-level investigations of oil/brine/rock interfacial interactions, driven by the surge in secondary and tertiary oil recovery technologies such as gas injection and chemical injection (Guo et al., 2022; Fan et al., 2024). Molecular dynamics simulation has revealed that salinity exerts a significant influence on rock-/oil interactions. In low-salinity systems, an electric double layer with repulsion effect forms at the rock/brine interface, whereas high-salinity ions tend to aggregate, assuming an anchoring role in oil adhesion to the carbonate surface (Koleini et al., 2020). Interestingly, it was found that adsorbed ion layers could have a screening effect on the adsorption of hydrocarbons onto the calcite surface (Chen et al., 2015). The disparity depends on the composition of the brine and oil components.

The focus of these studies primarily centered on the oil/brine interfacial interaction on carbonate surfaces, which have deepened our understanding to the microcosmic in-

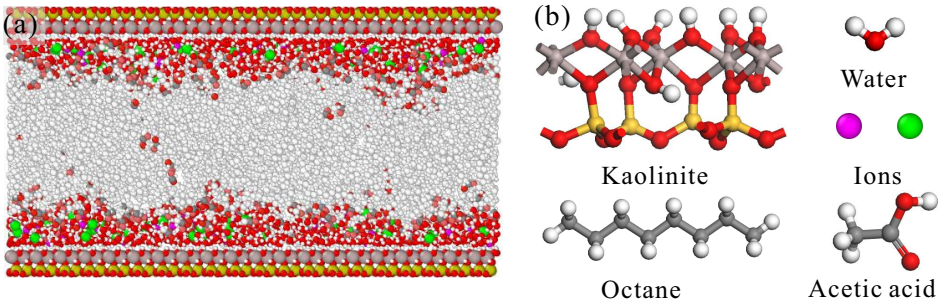

Fig. 2. (a) The simulation model of a kaolinite nanopore containing brine films and oil mixture and (b) the molecular models of kaolinite crystal, water, ions, octane and acetic acid molecules. The black, red, white, yellow, brown, pink, green spheres represent the carbon, oxygen, hydrogen, silicon, aluminum, sodium and chlorine atoms, respectively.

teraction behavior between ions and oil components within carbonate nanopores covered by brine films. Noticeably differs from carbonate minerals in terms of the chemical bonding mechanisms between polar oil components and surface chemical groups, clay minerals have stronger adsorption capability to polar oil components on the rock surface (Lin et al., 2018). Although there have been studies on the adsorption of oil components on clay surfaces with brine films (Zhang et al., 2019a), they mainly adopted an interfacial model consisting with aqueous solution and rock surface to study the static mechanism of oil/brine/rock interactions (Wei et al., 2017), neglecting the confined effect of nanopores and the dynamic flow behavior of crude oil. In fact, whether the spontaneous migration of crude oil under the pressure difference or miscible-phase oil displacement process by gas flooding or water flooding corresponds to a dynamic mechanism (Guo et al., 2020). The fluid properties such as density and viscosity can be influenced in the flow state, and the sticky and slippage effect can be pronounced (Zhang et al., 2019b; Liu et al., 2022). Consequently, greater attention should be directed towards the dynamic flow behavior of crude oil in nanopores covered with thin brine films. Furthermore, a comprehensive investigation covering interfacial interactions of oil/brine/rock and confined transport of crude oil in clay nanopores is fundamental both to oil/brine/rock interaction mechanisms and ion-engineered water flooding technology.

In this work, the static distribution characteristics and dynamic transport behaviors of oil mixture in kaolinite nanopores covered with different thin brine films are investigated by molecular dynamics simulation. The differences of the interaction modes between acetic acid molecules and ions at the oil-water interface are analyzed, and the interaction strength of acetic acid molecules with different ions is quantitatively calculated. The relationship between the interaction strength of single acetic acid molecules and ions is proved to be able to extend to illustrate the difference of oil flow behavior in nanopores. Furthermore, a strategy of displacing the binding sites of divalent cations with carboxylic acid by monovalent cations of a higher concentration is proposed. The feasibility of improving the oil mobility via cation exchange is further validated.

2. Molecular model and simulation methods

The simulation model is a slit pore constructed by two parallel substrates apart from a certain distance. The oil mixtures were located in the center of the pore and a brine film with a thickness around 0.55 nm were preplaced near the surfaces of both sides of the pore to simulate the formation water on the rock surfaces, as shown in Fig. 2(a). To simulate the high salinity solution environment of formation water in reservoir, the molarity of thin brine films is set as about 7.65 mol/L for the NaCl brine film system. When assessing the effect of individual ions, the corresponding counter ions are the same. The shale reservoir in Gulong area is abundant in clay minerals like kaolinite, montmorillonite and illite and so on. Considering the montmorillonite and illite crystals both contain free ions, which may influence the composition of brine films. Thus, the kaolinite was selected as the surface of the nanopore in this work, which is also widely existing in the sandstone and claystone reservoirs. In addition, the aluminol layer and siloxane layer of kaolinite are both typical base elements of clay minerals (Greathouse et al., 2017). Although the organic matter is also a significant composition of shale rock and has a strong interfacial adsorption for oil components, it is not suitable to be discussed in this work because of its intrinsic hydrophobicity. Crude oil is usually consisting of nonpolar and polar component. Nonpolar component is mainly hydrocarbon compound and polar component contains various heteroatom compound like carboxylic acids, phenols and amides (Lin et al., 2018). Generally, the molecular modeling of oil mixture can be based on the SARA model. However, considering the content of heavy fractions of shale oil in Gulong area is extremely low, and the oil density is also much lower than others. If oil mixture is constructed according to SARA model, the molecular model would be very large. On the other hand, considering the pivotal role of polar components in oil/brine/rock interactions, saturate aliphatic and carboxylic acid were selected as the representative of nonpolar and polar components of crude oil. Octane, as a common saturate aliphatic molecule, which was widely used as a representative components of shale oil (Wang et al., 2016), was selected as the nonpolar component of crude oil in this work. Carboxylic acid is a typical organic polar component in crude oil, which has been also confirmed as one of the

main polar components altering the surface wettability of minerals by experimental characterization methods such as X-ray diffraction spectroscopy and atomic force microscope (Pedersen et al., 2016). Herein, acetic acid, a simple carboxylic acid, was chosen to represent the polar oil component (Mahmoudvand et al., 2019). The oil mixture model constructed by saturate aliphatic and carboxylic acid molecules were also widely used in previous simulation studies (Underwood et al., 2016; Tian et al., 2018). In this work, the density of oil mixture is calculated as 0.775 g/cm^3 under the condition of 323 K and 30 MPa, which is also consistent with the characteristic of low density ($<$ 0.8 g/cm^3) of shale oil in Gulong area (Sun et al., 2021, 2023; He et al., 2023). The molecular model of kaolinite surface, water, ions, and oil molecules are displayed in Fig. 2(b).

To attain the initial model with a proper liquid density, an equivalent force to a typical reservoir pressure of 30 MPa along the direction perpendicular to surface is exerted on the atoms of the top kaolinite substrate. Once the system reached equilibrium, the top substrate was fixed at the equilibrium position, which is calculated by averaging the position in the last 1 ns. The pore height is defined as the distance between the nearest atoms of the top and bottom substrate, and the height of the slit pore in this work is 4.5 nm. Then equilibrium molecular dynamic simulation with duration of 15 ns were performed. After that, the non-equilibrium molecular dynamic simulation was carried out. The pressure gradient derives from the pressure difference of the two ends of nanopores. A simple method to achieve a pressure gradient is by setting two reservoirs with different pressure at the two ends of the nanopores (Jin et al., 2015). However, our work just employed a routine by exerting an equivalent constant acceleration to each atom of octane and acetic acid molecules along the Y direction to simulate a flow driven by pressure gradient (Chen et al., 2017; Yu et al., 2017). The system temperature was set at 323 K, which is in a representative reservoir temperature range and widely adopted in other studies (Fang et al., 2017). The temperature was controlled by the canonical ensemble and only the velocity components perpendicular to the flow direction was applied for the temperature thermostat. The time step for the velocity integration is 1 fs. The periodic boundary conditions were applied in the X and Y directions.

CHARMM-36 force field (MacKerell et al., 1998) was used to describe the intramolecular (bonds, angles and torsions) and intermolecular interactions among oil molecules, while the kaolinite surface was modeled by the CLAYFF force field (Cygan et al., 2004). The potential parameters of ions are derived from previous literature (Smith and Dang, 1994; Li and Merz, 2014; Williams et al., 2014), which were widely adopted in the study on oil/brine/rock interactions (Koleini and Badizad, 2019a). The TIP3P water model with a long-range Coulombic solver (Price and Brooks, 2004) was applied in our simulations, and the water molecules were set as rigid molecules. The non-bonding interactions were calculated by the 12-6 Lennard-Jones (LJ) and Coulomb potential (MacKerell et al., 1998):

$$E_{ij} = S(r_{ij}) \times 4\varepsilon_{ij}\left[\left(\frac{\delta_{ij}}{r_{ij}}\right)^{12} - \left(\frac{\delta_{ij}}{r_{ij}}\right)^{6}\right] + S(r_{ij}) \times \frac{q_i q_j}{4\pi\varepsilon_0 r_{ij}} \tag{1}$$

$$S(r_{ij}) = \frac{\left(r_{out}^2 - r_{ij}^2\right)\left(r_{out}^2 + 2r_{ij}^2 - 3r_{in}^2\right)}{\left(r_{out}^2 - r_{in}^2\right)^3} \tag{2}$$

where E represents the potential energy between two single particles, which were denoted as i and j; δ and ε is the zero-crossing distance and the LJ potential well depth; r is the distance between two particles; q is the particle charge; ε_0 is the vacuum dielectric constant and $S(r)$ is denoted as the energy switching function. The inner (r_{in}) and outer (r_{out}) cutoffs for the calculation of van der Waals and coulomb interactions are 8 and 12 Å, respectively. The long-range interactions were treated by the particle-particle particle-mesh solver with a precision of 10-4. The description of interactions between different types of particles was based on the Lorentz-Berthelot mixing rules. All of our simulations were run through Large-scale Atomic/Molecular Massively Parallel Simulator (Plimpton, 1995) and OVITO software (Stukowski, 2009) was used for the visualization and post-processing of simulation results.

3. Results and discussion

3.1 Density distributions

To investigate the effect of individual ions on the occurrence state and transport of crude oil in nanopores, four brine film systems was calculated, which are denoted as NaCl, $CaCl_2$, $MgCl_2$ and $MgSO_4$ brine film system according to the ion composition of brine films covered on the kaolinite surfaces. In general, interfacial adsorption phenomena occur for liquid molecules in nanopores due to their strong interfacial interactions (Hong et al., 2023). The disparity in interfacial adsorption is contingent upon the interaction strength between the liquid molecules and pore surfaces (Hong et al., 2022). Notably, a distinct interfacial layering phenomenon is observed among water, octane, and acetic acid molecules in the slit pores. Water molecules predominantly occupy the regions near the top and bottom surfaces, whereas octane molecules concentrate in the central area of the slit pores. Acetic acid molecules are primarily situated in the interfacial region between water and octane, assuming a linking role between the two phases, depicted in Figs. 3(a)-3(d). For different brine film systems, two structured hydration layers are formed on the kaolinite surface and the first density peak is much higher than the second layer, indicating a compact water monolayer are adsorbed on the kaolinite surface. The position and magnitude of density peak of water in four brine film systems is almost the same, indicating the ionic composition in brine films cannot disturb the hydration layers on the surfaces, which is consistent with the previous studies (Koleini and Badizad, 2019a). Turn to the density distribution of oil molecules, the octane molecules tend to be away the water molecules due to their hydrophobicity, and the disparity of density distribution in different brine film systems is small. It can be inferred that it is mainly because of the weak

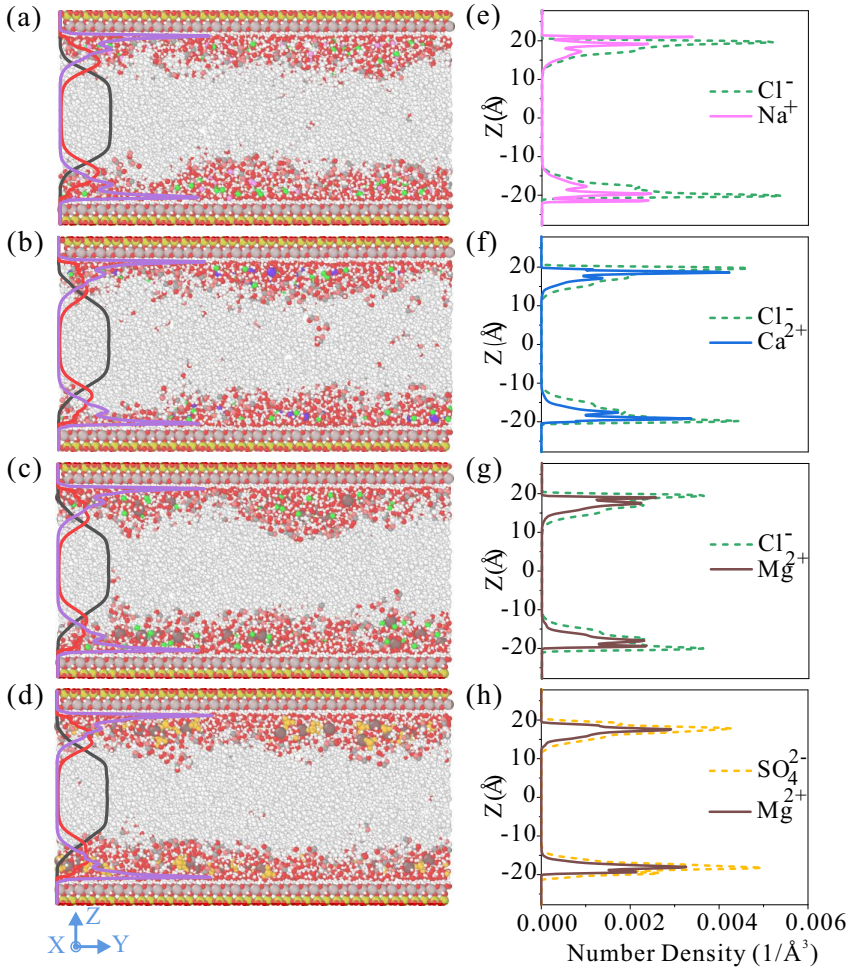

Fig. 3. (a)-(d) The density distributions and the simulation snapshots of oil components and water in NaCl, $MgCl_2$, $CaCl_2$ and $MgSO_4$ brine film systems, respectively; purple, black and red solid lines represent the density distribution profiles of water, octane and acetic acid, respectively, (e)-(h) the number density profiles of ions in NaCl, $MgCl_2$, $CaCl_2$ and $MgSO_4$ brine film system, respectively. To compare the distribution difference of cation and anion quantitatively, the number density has been normalized according to the molar concentration. Herein, the number density of sodium ion is the half of its actual number density for the comparison of cations, and the number density of sulfate ion is 2 times to its actual number density for the comparison of anions.

interactions between the ions in the brine film and octane molecules. Turning to the acetic acid, it can be seen that they are mainly adsorbed at the oil/brine interface, with the nonpolar methyl groups towards the side of octane molecules and polar carboxyl groups facing the side of brine films. In addition, when focused on the shape of density peaks, the density peak of $MgCl_2$, $CaCl_2$ and $MgSO_4$ brine film systems was found to be flatter and broader compared with that of the NaCl brine film system. Unlike the single peak of NaCl brine film system, the three brine film systems with divalent ions show a feature of weak double peaks, which is considered that there may be more than one interaction modes (Koleini et al., 2021) between acetic acid molecules and divalent ions.

Comparing the ion density profiles with the water density profiles, the distribution of monovalent sodium ions is also different from the brine film systems with divalent cations, shown in Figs. 3(e)-3(h). The density profile of sodium ions manifests three adsorption layers and the first Na^+ adsorption layer is in the first hydration layer, which means that the sodium ions have strong affinity to the kaolinite surface and some of them can penetrate the water monolayer. For the NaCl brine film system, the density peak of chloride ions in Fig. 3(e) is between the two density peak of sodium ions, implying that the absorption of chloride ions was dependent on the Na^+ adsorption layers (Badizad et al., 2021). Different from monovalent sodium ions, the divalent cations in $CaCl_2$ and $MgCl_2$ brine film systems are distributed in the region beyond the first hydration layer, which can be attributed to their more compact hydration shells for divalent cations than monovalent cations (Chen et al., 2015), displayed in Figs. 3(f) and 3(g). Accordingly, the monovalent chloride ions are more proximal to the kaolinite surface than divalent cations. By the comparison of the $MgCl_2$ and $MgSO_4$ brine film systems, the peak of sulfate ions is about 1.5 *Å* beyond that of chloride ions, which is possibly due to the larger size of polyatomic sulfate anion. In addition, the density peaks of sulfate ions and

magnesium ions in Fig. 3(h) are similar, which indicates the sulfate ions are inclined to adsorbed besides the magnesium ions rather than above them.

3.2 Impacts of brine ions on the oil flow

Taking account of the distinction between dynamic flow and static adsorption behavior of crude oil, our attention was turned to investigating the impact of brine films covering the kaolinite surface on the transport of oil through nanopores. Therefore, a pressure-driven flow was performed to investigate the flow behavior of oil components in nanopores with different brine films. There are five simulation systems in our simulation, named pure water film system, NaCl brine film, $CaCl_2$ brine film, $MgCl_2$ brine film and $MgSO_4$ brine film systems, respectively. The oil molecules in nanopores form a directional flow driven by the pressure gradient. The velocity profiles of oil molecules in five simulation systems are all parabolic, agreeing with the characteristics of Poiseuille flow. The oil velocity in the central region of the nanopores is followed by the order of pure water > NaCl > $CaCl_2$ > $MgCl_2$ > $MgSO_4$. Compared with four brine film systems, the oil velocity of pure water film system is much higher, which indicates that the ions in the brine film play an important role in the oil transport through nanopores. In addition, the impact of different ions in brine film on the oil flow is disparate, as displayed in Fig. 4(a). Especially, the velocity distribution at the oil/water interfacial region also varies in different systems. Because of the ion enrichment in the vicinity of surface, there is no interfacial slip happening at the oil/brine interface, which is similar with the sticky layer effect reported by the surface adsorption of heavy oil component (Hong et al., 2022). Inversely, the liquid/liquid slip at the oil/water interfacial region occurs in the pure water film system. This is because the first highly ordered water monolayer is tightly adsorbed on the hydrophilic kaolinite surface for the hydrogen bond interactions. The oil/water interaction is much weaker compared with oil/brine interaction and can even provide a lubrication effect (Guo et al., 2020). Hence, it can be concluded that the oil flow velocity in the proximity of the surface is contingent upon the interaction strength of oil/brine interface.

Considering that the polar acetic acid molecules are mainly concentrated at the oil/water interfacial regions, the oil molecules in close vicinity to the surfaces is thought to be affected most seriously by the brine film and also most difficult to move. Therefore, the velocities of oil molecules near the surfaces under different pressure gradient ranging from 0.01-9.7 MPa/nm were calculated to study the interfacial flow behavior of oil molecules. Herein, the oil molecules located within a 1 nm distance from the surface in the Z direction were considered to be in proximity to the surfaces. The oil velocity is determined by calculating the slope through linear fittings of the displacement (along the Y direction) versus time. Considering the thermal disturbance at the ultralow pressure gradients, when the oil velocity is below zero, the oil in the proximity to the surface was considered to have been not driven and its velocity was regarded as zero accordingly. With the augment of pressure gradient, the oil molecules at the oil/brine interface began to flow. The threshold pressure gradient refers to the minimum pressure required to drive the fluid to flow in low-permeability reservoirs, which can be measured by flow experiments (Hao et al., 2008) but its definition is still ambiguous at nanoscale, where the solid/liquid interface effect is predominant and there is a surface adsorption layer of liquids (Zhao, 2012). Herein, it was supposed that if the oil velocity in the vicinity of the surface is always more than zero above a pressure gradient, the corresponding pressure gradient was considered as the threshold pressure gradient. The threshold pressure gradient is a bit different for several simulation systems, depending the interaction intensity of oil/brine interface. The oil molecules near the surface in pure water film system begin to flow at the pressure gradient of about 0.1 MPa/nm and show a higher flow velocity than other brine film systems, as shown in Fig. 4(b). Comparatively, the oil in $MgCl_2$ and $MgSO_4$ brine film systems started to flow with requirement of a larger pressure gradient. Specifically, the oil velocities near the surfaces for brine film systems are in the order of $V_{NaCl} > V_{CaCl_2} > V_{MgCl_2} > V_{MgSO_4}$, which implies there is a consistent correlation between the oil velocity at the oil/brine interface and the central region in nanopores.

3.3 Interaction mechanisms

According to the preceding analysis, it was found that the acetic acid molecules are mainly residing at the oil/brine interfacial region, playing a linkage role between the nonpolar alkane and brine films, shown in Fig. 5(a). The acetic acid molecules can form various binding modes with the hydrated ions, which was also reported in previous studies (Underwood et al., 2015; Koleini and Badizad, 2019a). According to whether the acetic acid molecules bond with the ions directly or not, the binding modes between acetic acid molecules and ions can be mainly divided into two types: Direct binding and hydration bridging, displayed in Figs. 5(b)-5(e). It is worth noting that the donor atom of acetic acid molecule is different for cations and anions. The former tends to bond with carbonyl oxygen atom and the latter is inclined to hydroxyl hydrogen atom, which is derived from the charge difference of cations and anions.

To a certain extent, the interaction strength of the oil/brine interface directly influences the flow velocity of oil in nanopores. The interfacial interaction is mainly contingent on the strength of the interaction between the interfacial molecules in oil phase and brine phase. Considering the insensitivity of the alkanes to ion type (Cai et al., 1996), it can be speculated that the interaction strength of oil/brine interface primarily depends on the interactions between the acetic acid molecules and hydrated ions in brine films. Therefore, the calculation of the interaction strength between a single acetic acid molecule and a single hydrated ion was undertaken. In this computational model, the hydrated ion was immobilized at the central region of the kaolinite surface with a thin water film, while the acetic acid molecule was positioned directly above the ion. The initial distance between the donor atom (carbonyl oxygen or hydroxyl hydrogen) and the ion was

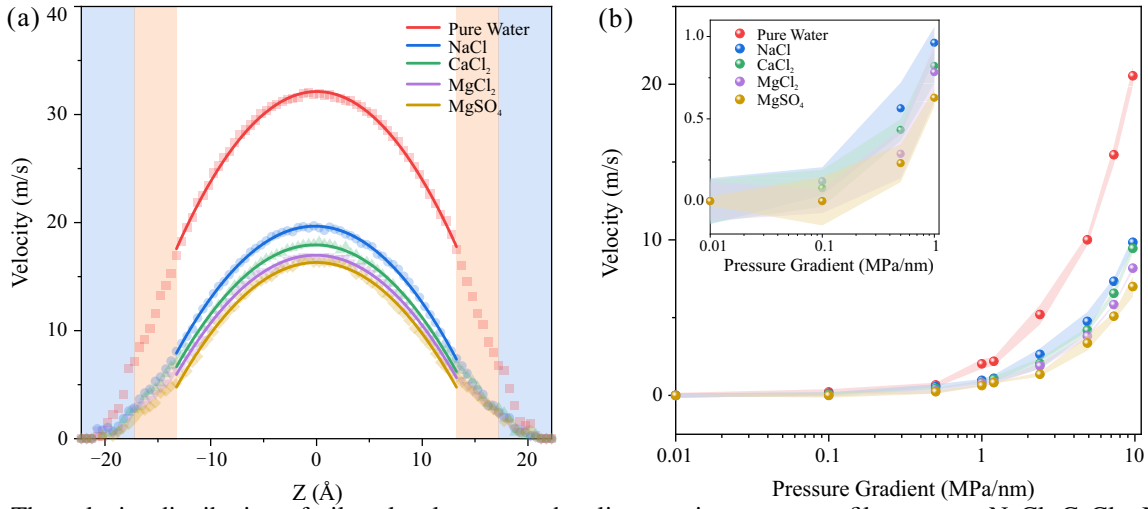

Fig. 4. (a) The velocity distribution of oil molecules across the slit pores in pure water film system, NaCl, $CaCl_2$, $MgCl_2$ and $MgSO_4$ brine film systems under the pressure gradient of 7.3 MPa/nm, represented by red, blue, green, purple and yellow dots, which are fitted by the corresponding solid lines. The light blue and orange regions represent the first and second hydration layers, respectively and (b) the velocities of oil molecules at the oil/brine interfacial region in different simulation systems with the pressure gradient. The inset is the enlarge figure of four brine film systems under the pressure gradients below 1 MPa/nm.

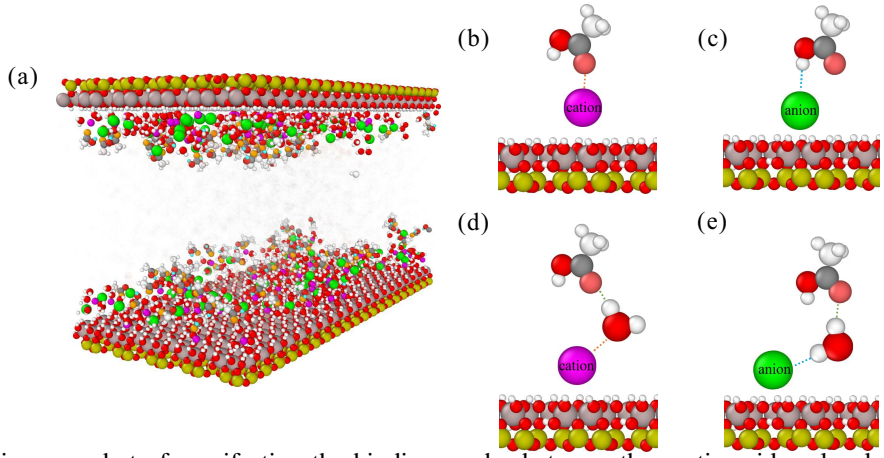

Fig. 5. (a) Simulation snapshot of manifesting the binding modes between the acetic acid molecules and ions at the oil/water interface. Direct binding mode for acetic acid molecules with (b) cations and (c) anions and hydration bridging mode for acetic acid molecules with (d) cations and (e) anions.

determined by the first peak of the radial distribution function. Subsequently, a spring force was applied to the methyl carbon atom of the acetic acid molecule, initiating its movement along the Y direction. To ensure a linear trajectory of the acetic acid molecule toward the ion, the degrees of freedom of the methyl carbon atom in the X and Z directions were constrained. This constraint aimed to allow the acetic acid molecules some freedom to adopt various binding modes with ions. The periodic boundary in the Y direction facilitated the repetitive interaction between acetic acid and ions. The total simulation time spanned 100 ns, during which the total force acting on the acetic acid molecule and the spring force were calculated over time. Correspondingly, the tangential force (F_y) along the Y direction of the acetic acid molecule was determined according to the total force and spring force. The distribution of tangential force of acetic acid molecules exhibits a general consistency with a Gaussian distribution. This Gaussian profile is not solely attributable to the random thermal motion of atoms but serves as an indication of more than one interaction mode, including both direct binding and hydration bridging. Typically, the interaction strength of direct binding exceeds that of hydration bridging, leading to the dominance of direct binding in the rightmost region of the force distribution profile, while the region near the peak is primarily contributed by hydration bridging. The force distribution of acetic acid molecules with divalent ions displays a broader span compared to that with monovalent ions, signifying a higher interaction intensity of direct binding with divalent ions than with monovalent ions, as illustrated in Fig. 6(a). Calculation of the average tangential force for acetic acid molecules with different cations and anions reveals a force hierarchy among cations: $Mg^{2+} > Ca^{2+} > Na^{+}$, and among anions: $SO_4^{2-} > Cl^{-}$, as depicted in Fig. 6(b), which is also consistent with previous experiment (Umadevi and

Senthilkumar, 2014) and first-principles calculations (Cui et al., 2023). This observation further substantiates the earlier assumption that the interaction intensity of the oil/brine interface is contingent on the binding strength between single acetic acid molecules and hydrated ions.

3.4 Feasibility analysis of cation exchange strategy

The interaction intensity between acetic acid molecules and different hydrated ions varies. When acetic acid molecules are coexisting with two different ions, a phenomenon of competitive binding between acetic acid and ions can occur. The ion with a stronger affinity for acetic acid exhibits preferential binding capabilities. Consequently, polar oil molecules tend to form binding structures with divalent or higher valence cations in the formation water system (Taylor and Chu, 2018). Furthermore, considering that a higher ion concentration can offer more ion binding sites for carboxylic acid, increasing the concentration of monovalent ions in the brine film can be a viable approach to replace divalent ions bound to carboxylic acid. To validate the aforementioned assumption, an ion exchange model to examine the competitive binding of Mg^{2+} and Na^{+} cations with acetic acid molecules was constructed. An acetic acid film, consisting of 200 acetic acid molecules, was situated above the kaolinite surface along with a brine film. The composition of brine films was meticulously designed, giving rise to four distinct sets of brine film systems. Among these, two were brine film systems with both Na^{+} and Mg^{2+} cations, featuring ion concentration ratios of (Mg^{2+}/Na^{+} = 1) and (Mg^{2+}/Na^{+} = 1/4), respectively. The other two brine films, each containing exclusively Mg^{2+} or Na^{+} cations, were computed for comparative analysis. Additional Cl^{-} anions were added to keep the system charge neutral in four brine film systems ($MgCl_2$/NaCl = 1, $MgCl_2$/NaCl = 1/4, $MgCl_2$ and NaCl systems).

Whether for the Mg^{2+} or Na^{+} cation, there are both two binding modes for the acetic acid molecule, as mentioned in Fig. 5, that is hydration bridging and direct binding. Therefore, the number of hydration bridging and direct binding for Mg^{2+} or Na^{+} cation in four brine film systems are calculated, shown in Fig. 7. The interaction mode of Mg^{2+} cations with acetic acid is predominantly characterized by hydration bridging. This arises from the compact hydration shell of Mg^{2+} cations, making it challenging for acetic acid molecules to penetrate. For Na^{+} cations, possessing a more loosely structured hydration shell, acetic acid molecules can readily penetrate and engage in direct binding with Na^{+} cation. As a result, both hydration bridging and direct binding are observed in abundance. When the concentration of Na^{+} ions is the same as the Mg^{2+} ions, there are even more Mg-hydrated bridging number for ($MgCl_2$/NaCl = 1) system compared with $MgCl_2$ system shown in Fig. 7(a), indicating that the Na^{+} cations cannot displace the binding sites of the acetic acid molecules with Mg_2^{+} cations. Inversely, whether the Na+-hydrated bridging mode or the Na^{+}-direct binding mode for NaCl system is reduced compared with the ($MgCl_2$/NaCl = 1) system, displayed in Fig. 7(b).

It shows that the binding sites of Na^{+} cations with the acetic acid molecules can be replaced by Mg^{2+} cations. Thus, it can be inferred that the competitive binding depends on the interaction strength with acetic acid when the concentration of two types of ions is the same. Once the concentration of Na^{+} cations is raised to 4 times to the Mg^{2+} cations, the number of Mg-hydrated bridging modes in ($MgCl_2$/NaCl = 1/4) system decreased substantially compared with $MgCl_2$ system, while the number of Na-hydrated bridging modes and Na-direct binding have been greatly enhanced than NaCl system. It indicates that some binding sites of Mg^{2+} cations with acetic acid molecules were replaced by Na^{+} cations when the concentration of Na^{+} cations is far higher than Mg^{2+} cations.

Therefore, a cation exchange mechanism can be interpreted, whose diagram schematic was displayed in Fig. 8. Initially, when the concentration of divalent cations is nearly equivalent to that of monovalent cations, the carboxylic acid molecule exhibits a preference for binding with the divalent cation due to its stronger adsorption capability, as depicted in Fig. 8(a). As more monovalent cations are introduced into the brine film, resulting in a significantly higher concentration of monovalent cations compared to divalent cations, as shown in Fig. 8(b), there are now more binding sites available for monovalent cations than divalent cations. During this phase, monovalent cations have a higher probability of binding with the carboxylic acid molecule and displacing the binding site of divalent cations, shown in Fig. 8(c). Once the carboxylic acid molecule binds with a monovalent cation, the divalent cations previously binding with carboxylic acid molecule are released from the surface, and the entire cation exchange process concludes, as displayed in Fig. 8(d).

3.5 Validation of cation exchange scheme

When the binding sites of divalent cations with acetic acid molecules are replaced by monovalent cations, the binding strength between the acetic acid molecule and hydrated ion can be weakened, thus the mobility of oil molecules should be enhanced. To further elucidate the relationship between the interaction strength of oil/brine interface and oil mobility through nanopores, a series of pressure-driven dynamic transport simulations were performed in the kaolinite nanopores with brine films containing varying Na^{+} displacement ratios to Mg^{2+} ions. The Na^{+} displacement ratio is defined as the difference between the initial system's Mg^{2+} number and the present system's Mg^{2+} number, divided by the initial system's Mg^{2+} number.

With the increasing Na^{+} displacement ratios, the volume flux of oil through nanopores has correspondingly increased, as depicted in Fig. 9(a). This indicates a rise in the amount of recoverable oil in nanopores, suggesting the potential for enhanced oil recovery. To quantitatively evaluate the impact of cation exchange on oil transport, the displacement efficiency η was defined by:

$$\eta = \frac{V_1 - V_0}{V_0} \tag{3}$$

where V_0 is the oil velocity of $MgCl_2$ brine film system, and

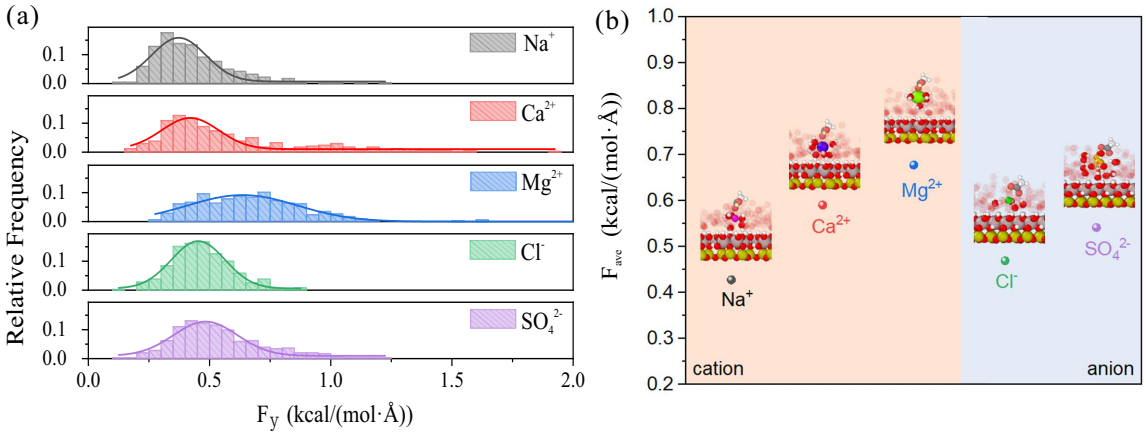

Fig. 6. (a) The frequency distribution histogram of tangential force of acetic acid molecule with different hydrated ions. The solid lines are the Gaussian fitting curves of the force distribution, where the Na^+, Ca^{2+}, Mg^{2+}, Cl^- and SO_4^{2-} are colored by the grey, red, blue, green and purple columns (lines), respectively and (b) the average tangential force of the acetic acid molecule to different hydrated ions, and the inset are molecular configurations of acetic acid molecule interacting with the hydrated ions, the left light orange region are three types of cations (Na^+, Mg^{2+}, Ca^{2+}) and the right light blue region are two types of anions (Cl^-, SO_4^{2-}).

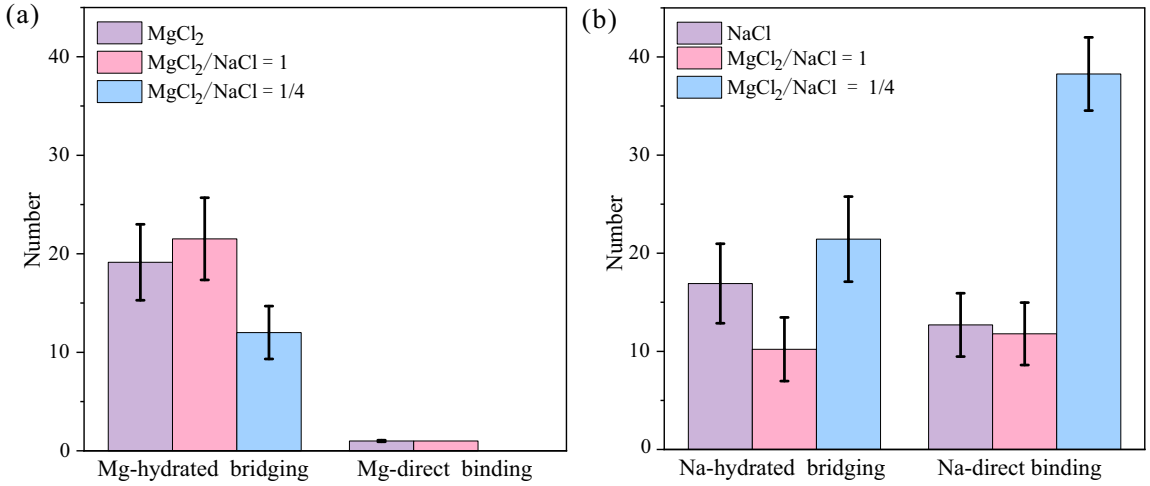

Fig. 7. (a) The number of Mg-hydration bridging and Mg-direct binding modes in different systems and (b) the number of Na-hydration bridging and Na-direct binding modes in different systems.

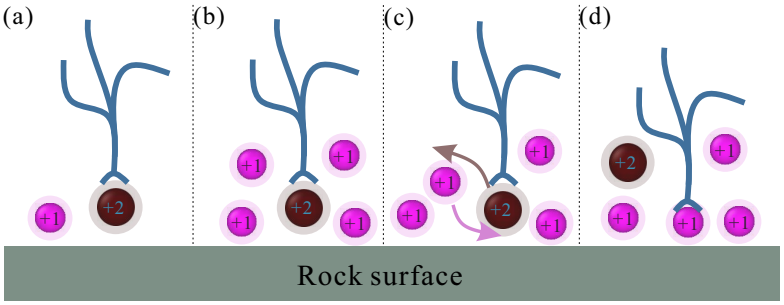

Fig. 8. The diagram schematic of using higher concentration monovalent cations to exchange the divalent cations binding with carboxylic acid. (a) Preferential binding of carboxylic acid with divalent cations when the concentration of monovalent cations is the same as the divalent cations, (b) More binding sites of monovalent cations compared with divalent cations after introducing monovalent cations with a higher concentration, (c) Monovalent cations are displacing the divalent cations binding with carboxylic acid at the advantage of concentration and (d) the divalent cation was completely exchanged by the monovalent cation and released from the surface.

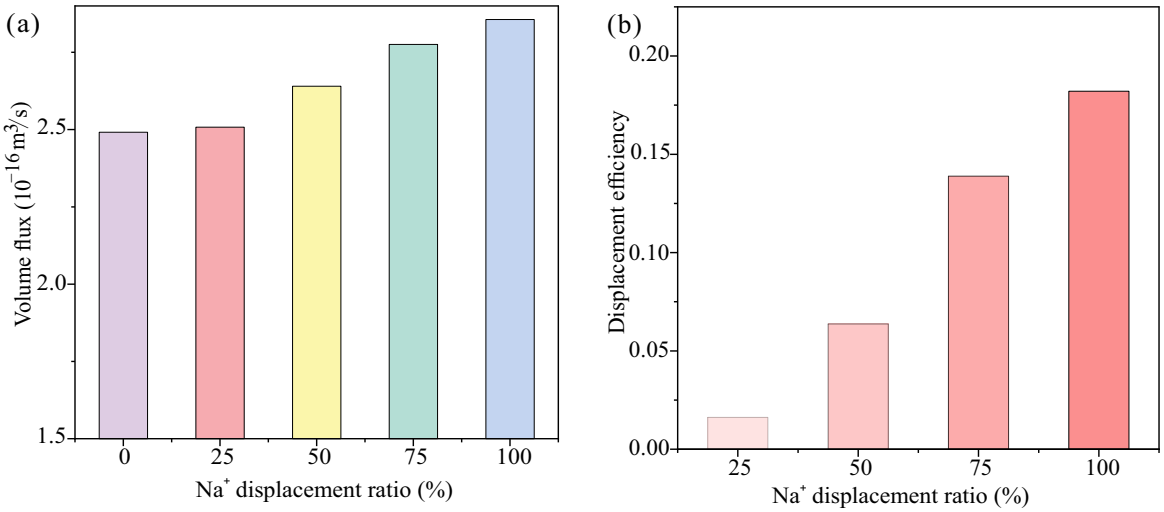

Fig. 9. (a) The volume flux and (b) the displacement efficiency of crude oil through kaolinite nanopores with different Na^+ displacement ratios at the pressure gradient of 7.3 MPa/nm.

the V_1 is the oil velocity of system after Na^+ cations displace the Mg^{2+} cations with different ratios.

It is observed that the displacement efficiency increases with the enhancement of Na^+ displacement ratios, shown in Fig. 9(b), indicating an improvement in the mobility of crude oil in nanopores. In other words, the replacement of divalent cations binding with carboxylic acid by monovalent cations can weaken the interaction intensity of the oil/brine interface, leading to an enhanced mobility of oil in nanopores.

3.6 Further discussions

Our study has provided valuable molecular insights into low salinity water flooding for kaolinite nanopores rich in acidic components. Previous studies have recognized both multicomponent ion exchange (Lager et al., 2008) and electrical double layer expansion (Ligthelm et al., 2009) as potential mechanisms of low salinity water flooding. In our study, when the concentration of Na^+ is equal to that of Mg^{2+}, there is no effective cation exchange to displace the binding sites of Mg^{2+} with carboxylic acid molecules, leading to a poor enhancement of oil recovery. This observation may appear contradictory to the multicomponent ion exchange mechanism of low salinity water flooding. However, it's essential to note that low salinity brine contains not only Na^+ and Cl^- but also several potential determining ions such as Ca^{2+}, Mg^{2+}, and SO_4^{2-}. Previous experiments have demonstrated that brine containing only NaCl cannot significantly alter rock wettability or increase an additional oil recovery (Moosavi et al., 2019; Koleini et al., 2021). Furthermore, it has been established that the injection of high salinity brine can greatly enhance oil recovery in secondary recovery processes (Al-Saedi et al., 2019). In addition, a previous study also introduced a direct correlation between oil-brine interfacial viscoelasticity and oil recovery from waterflooding, which further proved that high salinity brine has higher displacement efficiency than low salinity brine in smart waterflooding (Kar et al., 2022). These experimental findings align well with our simulations, emphasizing that for the cation exchange mechanism to be effective, a group of specific ions with competitive effect are required, rather than just a low salinity NaCl solution. However, it is important to note that rock/oil interactions and rock wettability are influenced by multiple comprehensive factors such as rock type, salt type and the composition of crude oil. Limited to the computation cost, this study specifically focuses on inorganic nanopores represented by kaolinite nanopores containing acidic oil components. Even so, it is believed that multi-component ion exchange mechanism exists widely in various reservoirs including carbonate and sandstone (Guo et al., 2020). The extent of the detailed mechanism varies, depending on the differences of interaction strength among polar oil components, rock surfaces and ions. Tailored to the specific reservoir characteristics, a scientifically designed injection brine is feasible for achieving additional oil recovery in ion-engineered water flooding.

4. Conclusions

In this study, the influence of brine films on the occurrence state and dynamic transport behavior of crude oil in kaolinite nanopores was examined. Polar acetic acid molecules exhibit a tendency to adsorb at the oil/brine interface, serving as a linking agent between the nonpolar alkane and brine films. The presence of brine films on kaolinite surfaces imparts an inhibitory effect on the transport of crude oil through nanopores. This inhibition can be attributed to the robust interfacial interaction between acetic acid molecules and hydrated ions at the oil/brine interface. The interaction modes between acetic acid molecules and ions was further analyzed, identifying both direct binding and hydration bridging modes for acetic acid molecules with cations and anions. The disparity between cations and anions was characterized by the difference in the donor atom of the acetic acid molecule. Calculations of the interaction intensity between a single acetic acid molecule and hydrated ions enabled the establishment of a relationship between interfacial interaction intensity and oil mobility in

nanopores. Additionally, a strategy involving the displacement of binding sites of divalent cations with carboxylic acid by monovalent cations of higher concentration was proposed. The feasibility of improving oil mobility through cation exchange was validated in independent oil transport cases. Our study not only demonstrates the effectiveness of the cation exchange mechanism in high salinity water flooding during secondary oil recovery from a molecular perspective but also offers crucial insights for low salinity water flooding. Specifically, our results suggest that a pure NaCl injection brine may not effectively exchange the divalent cations binding with polar oil components. It is believed that through the scientific design of injection brine, the multicomponent ion exchange mechanism can be harnessed to achieve additional oil recovery in ion-engineered water flooding whether in carbonate or sandstone reservoir.

Acknowledgements

This work was financially supported by the National Key Research and Development Program of China (No. 2019YFA0708700), the National Natural Science Foundation of China (Nos. U22B2075, 12241203 and 12102421), the Anhui Provincial Natural Science Foundation (No. 2108085QA39), and the Youth Innovation Promotion Association CAS (No. 2020449). The numerical calculations were performed on the supercomputing system in Hefei Advanced Computing Center and the Supercomputing Center of University of Science and Technology of China.

Conflict of interest

The authors declare no competing interest.

References

Al-Saedi, H. N., Alhuraishawy, A. K., Flori, R., et al. Sequential injection mode of high-salinity/low-salinity water in sandstone reservoirs: Oil recovery and surface reactivity tests. Journal of Petroleum Exploration and Production Technology, 2019, 9: 261-270.

Badizad, M. H., Koleini, M. M., Greenwell, H. C., et al. Atomistic insight into the behavior of ions at an oil-bearing hydrated calcite surface: Implication to ion-engineered waterflooding. Energy & Fuels, 2021, 35: 13039-13054.

Bai, S., Kubelka, J., Piri, M. Wettability alteration by smart water multi-ion exchange in carbonates: A molecular dynamics simulation study. Journal of Molecular Liquids, 2021, 332: 115830.

Buckley, J. S., Liu, Y. Some mechanisms of crude oil/brine/-solid interactions. Journal of Petroleum Science and Engineering, 1998, 20: 155-160.

Cai, B., Yang, J., Guo, T. Interfacial tension of hydrocarbon+water/brine systems under high pressure. Journal of Chemical & Engineering Data, 1996, 41: 493-496.

Cai, J., Zhao, L., Zhang, F., et al. Advances in multiscale rock physics for unconventional reservoirs. Advances in Geo-Energy Research, 2022, 6(4): 271-275.

Chakravarty, K. H., Fosbøl, P. L., Thomsen, K. Brine crude oil interactions at the oil-water interface. Paper SPE 174685 Presented at SPE Enhanced Oil Recovery Conference, Kuala Lumpur, Malaysia, 11-13 August, 2015.

Chen, H., Panagiotopoulos, A. Z., Giannelis, E. P. Atomistic molecular dynamics simulations of carbohydrate-calcite interactions in concentrated brine. Langmuir, 2015, 31: 2407-2413.

Chen, J., Yu, H., Fan, J., et al. Channel-width dependent pressure-driven flow characteristics of shale gas in nanopores. AIP Advances, 2017, 7: 045217.

Chu, W., Zhang, K. Fluid phase behavior of tight and shale reservoirs: Monte Carlo simulations. Advances in Geo-Energy Research, 2023, 7(2): 132-135.

Cui, F., Jin, X., Xia, J., et al. Micromechanical mechanism of oil/brine/rock interfacial interactions based on first-principles calculations. Journal of Molecular Liquids, 2023, 386: 122502.

Cygan, R. T., Liang, J. J., Kalinichev, A. G. Molecular models of hydroxide, oxyhydroxide, and clay phases and the development of a general force field. The Journal of Physical Chemistry B, 2004, 108: 1255-1266.

Denton, J. K., Kelleher, P. J., Johnson, M. A., et al. Molecular-level origin of the carboxylate head group response to divalent metal ion complexation at the air-water interface. Proceedings of the National Academy of Sciences of the United States of America, 2019, 116: 14874-14880.

Fan, J., Fan, J., Hong, X., et al. Exploring wettability variations on minerals surfaces: Insights from spreading coefficient and interaction energy analysis. Geoenergy Science and Engineering, 2024, 234: 212672.

Fang, T., Wang, M., Wang, C., et al. Oil detachment mechanism in CO_2 flooding from silica surface: Molecular dynamics simulation. Chemical Engineering Science, 2017, 164: 17-22.

Feng, Q., Xu, S., Xing, X., et al. Advances and challenges in shale oil development: A critical review. Advances in Geo-Energy Research, 2020, 4(4): 406-418.

Greathouse, J. A., Cygan, R. T., Fredrich, J. T., et al. Adsorption of aqueous crude oil components on the basal surfaces of clay minerals: molecular simulations including salinity and temperature effects. The Journal of Physical Chemistry C, 2017, 121: 22773-22786.

Guo, H., Nazari, N., Esmaeilzadeh, S., et al. A critical review of the role of thin liquid films for modified salinity brine recovery processes. Current Opinion in Colloid & Interface Science, 2020, 50: 101393.

Guo, H., Wang, Z., Wang, B., et al. Molecular dynamics simulations of oil recovery from dolomite slit nanopores enhanced by CO_2 and N_2 injection. Advances in Geo-Energy Research, 2022, 6(4): 306-313.

Hao, F., Cheng, L. S., Hassan, O., et al. Threshold pressure gradient in ultra-low permeability reservoirs. Petroleum Science and Technology, 2008, 26: 1024-1035.

He, W., Liu, B., Zhang, J., et al. Geological characteristics and key scientific and technological problems of Gulong

shale oil in Songliao Basin. Earth Science, 2023, 48(1): 49-62. (in Chinese)

Hong, X., Xu, H., Yu, H., et al. Molecular understanding on migration and recovery of shale gas/oil mixture through a pore throat. Energy & Fuels, 2023, 37: 310-318.

Hong, X., Yu, H., Xu, H., et al. Competitive adsorption of asphaltene and n-heptane on quartz surfaces and its effect on crude oil transport through nanopores. Journal of Molecular Liquids, 2022, 359: 119312.

Hu, Y., Chu, Z., Dai, C., et al. Probing of the hydrated cation bridges in the oil/brine/silica system via atomic force microscopy and molecular dynamics simulation. Fuel, 2021, 306: 121666.

Jiang, Q., Li, M., Ma, Y., et al. Molecular geochemical evaluation of shale oil mobility-A case study of shale oil in Jiyang depression. Petroleum Geology and Experiment, 2018, 6: 849-854. (in Chinese)

Jiang, Z., Li, T., Gong, H., et al. Characteristics of low-mature shale reservoirs in Zhanhua sag and their influence on the mobility of shale oil. Acta Petrolei Sinica, 2020, 41: 1587. (in Chinese)

Jin, Z., Firoozabadi, A. Flow of methane in shale nanopores at low and high pressure by molecular dynamics simulations. The Journal of Chemical Physics, 2015, 143(10): 104315.

Kar, T., Cho, H., Firoozabadi, A. Assessment of low salinity waterflooding in carbonate cores: Interfacial viscoelasticity and tuning process efficiency by use of non-ionic surfactant. Journal of Colloid and Interface Science, 2022, 607: 125-133.

Kilybay, A., Ghosh, B., Chacko, Thomas, N. A review on the progress of ion-engineered water flooding. Journal of Petroleum Engineering, 2017, 2017: e7171957.

Koleini, M. M., Badizad, M. H., Ayatollahi, S. An atomistic insight into interfacial properties of brine nanofilm confined between calcite substrate and hydrocarbon layer. Applied Surface Science, 2019a, 490: 89-101.

Koleini, M. M., Badizad, M. H., Hartkamp, R., et al. The impact of salinity on the interfacial structuring of an aromatic acid at the calcite/brine interface: An atomistic view on low salinity effect. The Journal of Physical Chemistry B, 2020, 124: 224-233.

Koleini, M. M., Badizad, M. H., Kargozarfard, Z., et al. The impact of salinity on ionic characteristics of thin brine film wetting carbonate minerals: An atomistic insight. Colloids and Surfaces A: Physicochemical and Engineering Aspects, 2019b, 571: 27-35.

Koleini, M. M., Badizad, M. H., Mahani, H., et al. Atomistic insight into salinity dependent preferential binding of polar aromatics to calcite/brine interface: Implications to low salinity waterflooding. Scientific Reports, 2021, 11: 11967.

Lager, A., Webb, K. J., Black, C. J. J., et al. Low salinity oil recovery-An experimental investigation. Petrophysics, 2008, 49(1): 28-35.

Li, P., Merz, K. M. Taking into account the ion-induced dipole interaction in the nonbonded model of ions. Journal of Chemical Theory and Computation, 2014, 10: 289-297.

Ligthelm, D. J., Gronsveld, J., Hofman, J. P., et al. Novel waterflooding strategy by manipulation of injection brine composition. Paper SPE 119835 Presented at the EUROPEC/EAGE Conference and Exhibition, Amsterdam, The Netherlands, 8-11 June, 2009.

Lin, M., Hua, Z., Li, M. Surface wettability control of reservoir rocks by brine. Petroleum Exploration and Development, 2018, 45: 145-153.

Liu, J., Yang, Y., Sun, S., et al. Flow behaviors of shale oil in kerogen slit by molecular dynamics simulation. Chemical Engineering Journal, 2022, 434: 134682.

MacKerell, A. D., Bashford, D., Bellott, M., et al. All-atom empirical potential for molecular modeling and dynamics studies of proteins. The Journal of Physical Chemistry B, 1998, 102: 3586-3616.

Mahmoudvand, M., Javadi, A., Pourafshary, P. Brine ions impacts on water-oil dynamic interfacial properties considering asphaltene and maltene constituents. Colloids and Surfaces A: Physicochemical and Engineering Aspects, 2019, 579: 123665.

Mohammed, M., Babadagli, T. Wettability alteration: A comprehensive review of materials/methods and testing the selected ones on heavy-oil containing oil-wet systems. Advances in Colloid and Interface Science, 2015, 220: 54-77.

Moosavi, S. R., Rayhani, M., Malayeri, M. R., et al. Impact of monovalent and divalent cationic and anionic ions on wettability alteration of dolomite rocks. Journal of Molecular Liquids, 2019, 281: 9-19.

Myint, P. C., Firoozabadi, A. Thin liquid films in improved oil recovery from low-salinity brine. Current Opinion in Colloid & Interface Science, 2015, 20: 105-114.

Pedersen, N. R., Hassenkam, T., Ceccato, M., et al. Low salinity effect at pore scale: Probing wettability changes in middle east limestone. Energy & Fuels, 2016, 30: 3768-3775.

Plimpton, S. Fast parallel algorithms for short-range molecular dynamics. The Journal of Chemical Physics, 1995, 117: 1-19.

Price, D. J., Brooks, C. L. A modified tip3p water potential for simulation with Ewald summation. The Journal of Chemical Physics, 2004, 121: 10096-10103.

Shaik, I. K., Song, J., Biswal, S. L., et al. Effect of brine type and ionic strength on the wettability alteration of naphthenic-acid-adsorbed calcite surfaces. Journal of Petroleum Science and Engineering, 2020, 185: 106567.

Smith, D. E., Dang, L. X. Computer simulations of NaCl association in polarizable water. The Journal of Chemical Physics, 1994, 100: 3757-3766.

Stukowski, A. Visualization and analysis of atomistic simulation data with OVITO-the open visualization tool. Modelling and Simulation in Materials Science and Engineering, 2009, 18: 015012.

Sun, L., Cui, B., Zhu, R., et al. Shale oil enrichment evaluation and production law in Gulong Sag, Songliao Basin, NE China. Petroleum Exploration and Development, 2023, 50(3): 505-519.

Sun, L., Liu, H., He, W., et al. An analysis of major scientific

problems and research paths of Gulong shale oil in Daqing Oilfield, NE China. Petroleum Exploration and Development, 2021, 48(3): 527-540.

Taylor, S. E., Chu, H. T. Metal ion interactions with crude oil components: Specificity of Ca^{2+} binding to naphthenic acid at an oil/water interface. Colloids and Interfaces, 2018, 2: 40.

Tian, S., Erastova, V., Lu, S., et al. Understanding model crude oil component interactions on kaolinite silicate and aluminol surfaces: Toward improved understanding of shale oil recovery. Energy & Fuels, 2018, 32: 1155-1165.

Umadevi, P., Senthilkumar, L. Influence of metal ions (Zn^{2+}, Cu^{2+}, Ca^{2+}, Mg^{2+} and Na^{+}) on the water coordinated neutral and zwitterionic L-histidine dimer. RSC Advances, 2014, 4: 49040-49052.

Underwood, T., Erastova, V., Cubillas, P., et al. Molecular dynamic simulations of montmorillonite-organic interactions under varying salinity: An insight into enhanced oil recovery. The Journal of Physical Chemistry C, 2015, 119: 7282-7294.

Underwood, T., Erastova, V., Greenwell, H. C. Wetting effects and molecular adsorption at hydrated kaolinite clay mineral surfaces. The Journal of Physical Chemistry C, 2016, 120: 1143349.

Wang, F., Wu, H. Molecular dynamics studies on spreading of nanofluids promoted by nanoparticle adsorption on solid surface. Theoretical and Applied Mechanics Letters, 2013, 3: 054006.

Wang, H., Cai, J., Su, Y., et al. Pore-scale study on shale oil-CO_2-water miscibility, competitive adsorption, and multiphase flow behaviors. Langmuir, 2023, 39, 34, 12226-12234.

Wang, S., Javadpour, F., Feng, Q. Molecular dynamics simulations of oil transport through inorganic nanopores in shale. Fuel, 2016, 171: 74-86.

Wang, X., Xiao, S., Zhang, Z., et al. Displacement of nanofluids in silica nanopores: Influenced by wettability of nanoparticles and oil components. Environmental Science: Nano, 2018, 5: 2641-2650.

Wei, B., Wu, R., Lu, L., et al. Influence of individual ions on oil/brine/rock interfacial interactions and oil-water flow behaviors in porous media. Energy & Fuels, 2017, 31: 12035-12045.

Williams, C. D., Burton, N. A., Travis, K. P., et al. The development of a classical force field to determine the selectivity of an aqueous Fe^{3+}-EDA complex for $TcO^{4-}$and $SO_4{}^{2-}$. Journal of Chemical Theory and Computation, 2014, 10: 3345-3353.

Wu, Z., Sun, Z., Shu, K., et al. Mechanism of shale oil displacement by CO_2 in nanopores: A molecular dynamics simulation study. Advances in Geo-Energy Research, 2024, 11(2): 141-151.

Yu, H., Chen, J., Zhu, Y., et al. Multiscale transport mechanism of shale gas in micro/nano-pores. International Journal of Heat and Mass Transfer, 2017, 111: 11721180.

Zhang, H., Jiang, Y., Zhou, K., et al. Connectivity of pores in shale reservoirs and its implications for the development of shale gas: A case study of the lower Silurian Longmaxi formation in the southern Sichuan basin. Natural Gas Industry B, 2020, 7: 348-357.

Zhang, L., Lu, X., Liu, X., et al. Distribution and mobility of crude oil-brine in clay mesopores: Insights from molecular dynamics simulations. Langmuir, 2019a, 35: 14818-14832.

Zhang, W., Feng, Q., Wang, S., et al. Oil diffusion in shale nanopores: insight of molecular dynamics simulation. Journal of Molecular Liquids, 2019b, 290: 111183.

Zhao, Y. P. Physical Mechanics of Surfaces and Interfaces, Beijing, China, Science Press, 2012. (in Chinese)

Zou, C., Zhu, R., Bai, B., et al. Significance, geologic characteristics, resource potential and future challenges of tight oil and shale oil. Bulletin of Mineralogy Petrology and Geochemistry, 2015, 34(1): 3-17. (in Chinese)